# Videometrics IV

# Zoom lens calibration for wind tunnel measurements

A. W. Burner

NASA Langley Research Center MS 236
Hampton, VA 23681-0001
Tel: 804 864 4635, Fax: 804 864 7607, email: a.w.burner@larc.nasa.gov

## ABSTRACT

This report summarizes an investigation of zoom lens calibration, with emphasis on the effects of lens-image-plane misalignment. Measurements have been made of the photogrammetric principal point and radial (symmetrical) and decentering (asymmetrical) distortion components as a function of the principal distance (zoom setting) of several zoom lenses. Data were also taken with the axis of symmetry (optical axis) of a zoom lens aligned and misaligned to the same solid-state video camera. An explanation is offered regarding the variation of the principal point as a function of zoom setting based on these measurements. In addition the relationship of the decentering distortion to radial distortion, principal distance, and lens-image-plane misalignment angle is discussed. A technique for determining the proper point of symmetry to be used for distortion computations (as opposed to the principal point) is also suggested. A simple technique for measuring the misalignment angle of zoom lenses when attached to video cameras is presented, along with measurements for seven solid-state cameras. A method to reduce the additional error introduced by zoom lens misalignment is presented. The implications of this study are that special measures to properly align a zoom lens to the sensor image plane are probably not necessary, but that as the accuracy obtainable in digital photogrammetry approaches the 0.01 or less pixel level, additional calibration including the point of symmetry for distortion computation should be considered.

**Keywords**: calibration, zoom lenses, decentering distortion, asymmetrical distortion, misaligned image plane, point of symmetry, video cameras, CCD, wind tunnel.

## 1. INTRODUCTION

The variable field of view of a zoom lens can be advantageous in wind tunnel applications using video cameras. These applications include wind tunnel model attitude and position, model deformation (e.g., wing twist and bending), and qualitative and quantitative flow visualization of various flow field parameters. However, a varying field of view is an additional complication which must be accounted for in close-range photogrammetric measurements. In some wind tunnels, especially high-pressure cryogenic wind tunnels, video cameras are located in pressure vessels and are not routinely available for lab calibration. In addition, the dynamic nature and camera location restrictions of wind tunnel testing preclude the use of self calibration during data taking so that pre- or post-test calibration of the zoom lens is necessary. Previous calibrations of zoom lenses[1,2] have shown that the photogrammetric principal point (PPP) often varies linearly with zoom setting and that the distortion characteristics also change with zoom setting. It was also determined that the changes for a given camera-lens combination were systematic and stable over time.

## 2. LENS-IMAGE-PLANE MISALIGNMENT

### 2.1. Background

The fundamental reference to be used in the collinearity equations is discussed in early photogrammetric literature such as Ref. 3 where it is stated (after mentioning principal point and principal distance) that, "These terms are standard ones long used in the theory of perspective and are applicable to any representation in perspective, whether it is a photograph, painting, or drawing. It will be noted that the definitions are in **terms of the photograph and bear no reference to the camera**", (emphasis added). In Ref. 4 it is stated that the collinearity equations "...relate the two dimensional, measured coordinates $x, y$, of an image and the corresponding three dimensional spatial coordinates $X, Y, Z$ of the point photographed...the camera is idealized as consisting of but two essential elements: a center of projection $C$ (an abstraction of the lens) and a photographic or image plane...". Note that in Refs. 3 and 4 it is the image plane and its relation to the perspective center (center of projection) which is of fundamental importance rather than the relation of the image plane to the

optical axis. Note also that collinearity applies to a pinhole camera in which an optical axis has no meaning. Thus the fundamental reference in the collinearity equations is the image plane, not the optical axis of the lens. Since the image plane and not the optical axis is the fundamental reference, so long as the principal point is correctly interpreted to be the foot of the perpendicular from the rear perspective center on the image plane and not the intersection of the optical axis, collinearity must hold, **even** for an image plane which is angularly misaligned to the optical axis (provided no radial distortion is present which would also invalidate collinearity for an image plane which is **not** misaligned). Also note that collinearity can be used to transform from a properly aligned image plane to a misaligned image plane. This transformation can be simplified and expressed as a 2-D projective transformation.

If radial distortion is present, the location on the image plane for zero distortion does not occur at the photogrammetric principal point (PPP) for misaligned image planes, but instead occurs at the intersection of the optical axis and image plane (which can be thought of as the point of symmetry). This point of symmetry is the proper reference to be used for distortion computations. The use of two separate reference points, one for imaging with collinearity (the PPP) and one for distortion computations (the point of symmetry) is discussed in Refs. 5 and 6. Reference 7 has a brief explanation that the two points do not coincide if the image plane is not perpendicular to the optical axis and that the misalignment of the image plane can be found as the arctangent of the distance between the two reference points divided by the principal distance.

## 2.2. Lens-image-plane misalignment relationships

In the following an ideally constructed lens is assumed. All centers of curvature of the various lens surfaces which make up the lens are assumed aligned along a common axis referred to here as the optical axis of the lens. Such a perfectly constructed lens with optical axis perpendicular to the image plane would have no decentering distortion, but might still suffer from radial distortion. It is the combination of a perfectly constructed lens and an angularly misaligned image plane which is the subject of this discussion. For the perfectly constructed lens, the undistorted image plane coordinates are given by the intersection in the image plane of a ray from a given object point which enters the lens at the front perspective center and exits the lens at the rear perspective center on its way toward the image plane. This relationship is described with the collinearity equations. Complications due to pupils are not considered here. Radial distortion is considered to be a function only of the undistorted image coordinates on an image plane which is perpendicular to the optical axis and therefore, with this model, the radial distortion would not vary with object distance for a fixed principal distance.

For a misaligned image plane and ideally constructed lens the photogrammetric principal point used in imaging relationships (collinearity) is not located at the intersection of the optical axis with the image plane, but rather at the intersection of a perpendicular from the rear perspective center to the image plane. Instead, the intersection of the optical axis with the image plane locates the proper point of symmetry to be used in the computation of distortion corrections. The variation of the location of the principal point, $x_p, y_p$, as the lens is shifted along the optical axis (mimicking a zoom lens) is depicted in Fig. 1. In Fig. 1 the front and rear perspective centers have been collapsed into a single perspective center as in the thin lens approximation. The point of symmetry $x_s, y_s$ remains fixed while the principal point, being defined as the foot of the perpendicular to the image plane from the rear perspective center, varies with zoom setting.

In analytical self-calibration only one *principal* point can generally be solved for. If radial distortion is zero this single point will correspond to the PPP, even if the image plane is misaligned. For a misaligned image plane when radial distortion is present, the single point found will approximate the PPP, but may have some additional error due to competition in the solution between imaging, which is based upon the PPP, and lens distortion, which is minimized by reference to the displaced point of symmetry. The collinearity equations are fully applicable to misaligned image planes without radial distortion as discussed above. When comparing image coordinates of an aligned and a misaligned image plane there will be an *apparent* distortion which is analogous to the *apparent* distortion between two images (neither of which suffers any lens distortion) of an object from different perspectives. For an ideally constructed lens without radial distortion, no distortions are introduced if the image plane is not perpendicular to the optical axis of the lens.

As mentioned above, a 2-D projective transformation can be used to create the projective equivalent of a misaligned image plane from aligned image data. Given an image point and the rear perspective center and the straight line propagation of light (at least in this completely geometrical model) the conditions of collinearity are met. In other words, we can treat any image point as being an object point for another image plane (actual or theoretical), even if that plane happens to be tilted. For example, we can consider all the image points on the ideal image plane to be an object target field with $Z = 0$, and $X, Y$ given

by the image plane coordinates with respect to the optical axis. The rotation of the new image plane with respect to the ideal perpendicular image plane in the standard $\omega$, $\phi$, $\kappa$ system may then be given by $\omega$, $\phi$, 0. (The $\kappa$ rotation is unimportant here and is arbitrarily set to 0.) The principal distance for the new image plane is taken to be equal to the same value as for the ideal image plane, $c$, with the perspective center located at 0, 0, $c$. If a different principal distance is used, the distortion (assuming that we are using the usual spatial description of distortion and not the angular description which is independent of principal distance) will have to be scaled inversely with the square of the new principal distance. We then simply apply the collinearity equations to determine the image locations on the new image plane. The necessary 2-D projective equations to perform this transformation are thus derivable from the 3-D collinearity equations.

Possible fallacies in this model are that the perspective center may not be independent of image location for real systems and that the centroid of the image location may change with varying image plane positions so that the central ray of the image is not entirely adequate to define the image location on a new image plane. These fallacies are believed to be small effects on an already small effect and probably negligible. Thus an excellent model would appear to be the collinearity equations (or equivalent 2-D projective equations) for the transformation from ideal to misaligned image plane.

Self-calibrations were conducted comparing simulated data from an aligned and misaligned lens. Denoting the point of symmetry by $x_s$, $y_s$ (intersection of optical axis of the lens with the image plane) and the principal point by $x_p$, $y_p$ (foot of perpendicular from rear perspective center) we have the following relationships based on geometry

$$\omega = \tan^{-1}\left(\left(y_p - y_s\right)/c\right)$$

$$\phi = \tan^{-1}\left(\left(x_s - x_p\right)/c\right)$$

(1)

where $\omega$ is the + ccw rotation of the image plane about the $x$-axis and $\phi$ is the + ccw rotation of the image plane about the $y$-axis. Further simplifications occur by dropping the $\tan^{-1}$.

Self-calibration simulations which allow for a principal point, but no point of symmetry, indicate that if the aligned image data have no radial distortion, the transformed misaligned image data also will have no radial or decentering distortion. If the aligned image data have radial distortion, the transformed misaligned image data not only have the approximate same value of radial distortion as the aligned data, but, in addition, have nonzero values for the decentering distortion parameters $P_1$ and $P_2$. Simulations show that $P_1$ and $P_2$ correct for most of the additional distortion (which is found to be directly proportional to the radial distortion) introduced by the misaligned image plane.

When the principal point only is used as the single point of reference for collinearity and distortion computations, $P_1$ and $P_2$ are found to be approximately directly proportional to the third order radial distortion $K_1$, angles of misalignment $\omega$ and $\phi$ (about horizontal and vertical image plane axes), and principal distance $c$ as follows

$$P_1 = \phi \ c \ K_1$$

$$P_2 = -\omega \ c \ K_1$$

(2)

where $\omega$ and $\phi$ are, of course, in radians. Note that these relations are dimensionally correct and yield estimates of $P_1$ and $P_2$ in good (10%) agreement for a simulation with $c = 75$ mm, $\omega = \phi = 0.5$ deg, and $K_1 = 1.3 \times 10^{-3}$ mm$^{-2}$. Equations (2) are approximate since the profile function used in the original derivation of $P_1$ and $P_2$ was truncated to second order.

The dependence of the decentering parameters on the principal distance is mentioned in Ref. 8, although it appears that the dependence described there is an inverse dependence rather than a direct dependence as presented here. The dependence of the decentering aberrations on the radial distortion is mentioned in the original Conrady reference published in 1919[9]. These dependencies have apparently received little attention in the photogrammetric literature. There are several interesting implications due to these proportionalities. For instance, these proportionalities are in complete agreement with the statement that the collinearity equations hold for misaligned image planes which have no radial distortion since the misaligned image data with zero radial distortion will also have zero values of $P_1$ and $P_2$, independent of the misalignment angle.

According to equations (2) the decentering distortion terms $P_1$ and $P_2$ are equal to zero at a principal distance, $c$, of zero. Thus, from equations (3), the point of symmetry and the PPP must coincide at $c = 0$ where $P_1 = P_2 = 0$. The point of symmetry for a zoom lens can also be found by noting the stationary point on the image plane while zooming the lens. The point of symmetry found in this manner has sometimes been used incorrectly as the principal point.

If the principal point location, radial, and decentering distortion have been determined from self-calibration then from equations (3) the location of the point of symmetry can be estimated with data which does not even consider the existence of the point of symmetry explicitly. With this estimate of $x_s, y_s$ the self-calibration (or plumb line calibration) could be repeated, but this time with $x_s, y_s$ treated as constant and used for distortion corrections instead of $x_p, y_p$. Several iterations should yield an improved (but possibly only marginally) calibration with smaller values of $P_1$ and $P_2$ for cases in which lens-image-plane misalignment is significant.

# 3. EXPERIMENTAL MEASUREMENTS OF ZOOM LENSES

## 3.1. Principal point and point of symmetry

Five zoom lenses were tested for the variation of the principal point with zoom setting (principal distance). One Sony zoom (12.5 to 75 mm fl), one Angenieux zoom (20 to 80 mm fl), and three zooms from Canon (10 to 100 mm, 17 to 102 mm, and 15 to 150 mm fl) were tested. A laser illumination technique described in Ref. 7 was use to determine the variation of the principal point with zoom setting. In this technique a laser is aligned to be perpendicular to the CCD sensor without a lens present. The lens is them replaced and, after proper filtering, the centroid of the laser spot is recorded as a function of zoom setting. The variations of the principal points in $x$ and $y$ were found to be very linear and repeatable with zoom setting for all but the Angenieux zoom. The optical elements of the Angenieux zoom rotate as the zoom setting is changed, unlike the other four zooms for which the optical elements slide along the optical axis as the zoom setting is varied, closely following the model presented above. Note that the weight of large zoom lenses may change the no-load angular orientation of the $c$ mount of the video camera in relation to the sensor image plane causing a shift in the $y$-values of the PPP and point of symmetry since the perspective center may be displaced and the optical axis may intercept the image plane displaced in $y$.

The pixel variation of the photogrammetric principal point (PPP) with zoom setting is plotted in Fig. 2 for the Sony zoom lens. The location of the point of symmetry at the zero intercept as illustrated was found to agree within a few pixels to the point of symmetry found by imaging as well as to the point of symmetry found with the laser illumination technique when aligned with the mechanical axis of the zoom as described in Ref. 7. From equations (1) the magnitudes of the misalignment angles $\omega$ and $\phi$ are equal to the arctangent of the slopes of these plots after converting to units of length. For this particular zoom lens camera combination the misalignment angles about the horizontal ($\omega$) and vertical ($\phi$) axes were found to be $-0.41°$ and $0.53°$ respectively with equations (1). The same zoom lens was used with several solid state cameras in order to determine the range of likely misalignment angles. Measurements of the lens-image-plane resultant misalignment angle for seven other solid-state cameras using this technique ranged from $0.15°$ to $0.53°$ with a mean of $0.36°$.

## 3.2. Lens-image-plane misalignment experiment

In order to compare calibration results with and without misalignment the following experiment was conducted. The Sony zoom lens was mounted separately from a solid state CID sensor such that the optical axis of the zoom lens could be aligned independently of the image plane of the sensor. The zoom lens was aligned initially so that the optical axis of the zoom was perpendicular to the sensor image plane. This was accomplished by positioning the optical axis so that the variation in principal point over the entire range of zoom focal length setting was less than a few pixels. The optical axis of the zoom lens was later rotated $0.5°$ in the horizontal and vertical directions to establish a known lens-image-plane misalignment. Optical bench calibrations described in Ref. 7 were made of the horizontal and vertical pixel spacing and sensor axis non-perpendicularity and used throughout the test. Measurements were then made of the principal point variation, point of symmetry, and the usual five distortion coefficients (three radial and two decentering) at various zoom settings for the aligned and misaligned cases. The seventh order radial distortion was found to be insignificant upon comparison to its computed standard deviation for all cases and is excluded from further analyses.

Uncorrected and corrected image plane distortion residuals for the aligned and misaligned cases are presented in Figs. 3 and 4 respectively covering a range of zoom lens focal length settings from 12.5 to 75 mm. A nearly planar target field in an

optical bench experimental arrangement similar to that described in Ref. 7 was used to determine the distortion. The density of the retroreflective targets was doubled near the center of the target plate to better accommodate the longer focal length settings of the zoom. Distortion corrections consisted of third and fifth order radial distortion $K_1$ and $K_2$, and decentering distortion $P_1$ and $P_2$. A single point of symmetry, as described above, was used for each case.

The residuals before correction are similar for both the aligned and misaligned cases. One can not judge by the residual plots which one had the optical axis misaligned to the image plane. Similar results are noted for the corrected residuals. A slight reduction in residuals, however, may be noted at the shorter focal settings for the misaligned case and is more obvious in Fig. 5 which plots the rms image plane residuals versus zoom setting for the aligned (circles) and misaligned (squares) cases. The rms image plane residuals are plotted again in Figs. 6 and 7 to illustrate the increase in residuals when the nominal center of the sensor (denoted by triangles) is used in the distortion computation as opposed to the experimentally determined point of symmetry (denoted by circles for the aligned case and by squares for the misaligned case). In both cases the use of the measured point of symmetry reduces the magnitude of the residuals, especially for large values of the zoom setting.

The third ($K_1$) and fifth ($K_2$) order radial distortion terms are plotted versus zoom setting in Fig. 8 with the circles and squares representing the aligned and misaligned cases respectively for this and succeeding applicable figures. Error bars representing ±2 standard deviations computed from the least squares adjustment are plotted if greater than the symbol size for this and succeeding figures. The smoothly varying systematic nature of the $K_1$ plot and the reduction of $K_1$ to zero at a small focal length are very similar to results found by others[1]. The differences of the radial distortion coefficients between the aligned and misaligned cases are plotted in Fig. 9 where the error bars represent twice the root sum square of the computed standard deviation for each case. The differences between the aligned and misaligned cases are only slightly significant.

Similar plots for decentering distortion, $P_1$ and $P_2$ are presented in Figs. 10 and 11. For the ideally constructed lens with optical axis parallel or misaligned to the image plane, $P_1$ and $P_2$ should be zero provided the correct point of symmetry is used in the distortion computations. The nonzero values in Figs. 10 and 11 may indicate decentering errors in the zoom lens itself. Figures 12 and 13 compare results for the aligned case when using the measured point of symmetry (denoted by circles) and the nominal center of the image plane (denoted by triangles) for distortion computations for the two coefficients of radial distortion and two coefficients of decentering distortion. Similar plots for the misaligned case are presented in Figs. 14 and 15. Little effect is noted on radial distortion for either case except at the longer focal lengths. However, a noticeable increase in the magnitude of the decentering coefficients is observed if the measured point of symmetry is replaced with the nominal center of image plane. Note that the decentering distortion results using the measured point of symmetry and the nominal center of the image plane coincide near the focal length setting where $K_1$ passes through zero.

As a final example, the effect of variations from the measured point of symmetry on optical bench distortion computations are presented at a nominal zoom focal setting of 30 mm for the aligned case. Figure 16 shows the rms image plane residuals from the distortion computation versus deviation from the measured point of symmetry in the $x$ and $y$ directions in pixels. Note that the residuals are relatively insensitive to changes in the point of symmetry over ±25 pixels or so, indicating that very accurate measurements of the point of symmetry may not be necessary in some cases. Figures 17, 18, 19, and 20 show the effect on radial and decentering distortion. The third ($K_1$) and fifth ($K_2$) order radial distortion have a minimum or maximum at the measured point of symmetry whereas the decentering terms $P_1$ and $P_2$ are only sensitive to changes in the $x$ and $y$ values respectively of the point of symmetry. This single axis sensitivity of the decentering distortion terms is generally well known.

## 4. RECOMMENDATION

Additional studies are needed on the self-calibration of aligned and misaligned zoom lenses, perhaps combined with plumb line calibrations, to determine the value of using a separate point of symmetry for distortion computations in an iterative manner during self-calibration. Provided a separate point of symmetry is of value, tests need to be conducted comparing the laser illumination measurement of the variation in principal point and corresponding point of symmetry to the use during self-calibration of the relations presented above for lens-image-plane misalignment.

## 5. SUMMARY

Measurements of the photogrammetric principal point as a function of the principal distance (zoom setting) of several zoom lenses have been made. Symmetrical (radial) and asymmetrical (decentering) distortion components have also been measured as a function of zoom setting. The linear variation of the principal point and the variation in distortion components as a function of zoom setting are in agreement with studies made by others. It is suggested that the linear variation of principal point is due to misalignment of the axis of symmetry of the zoom lens to the sensor image plane and that the proper point of symmetry to be used for distortion computations can be found as the intercept at zero principal distance. One should consider using a common point of symmetry for distortion computations at all zoom settings, but a linearly varying (with zoom setting) principal point in photogrammetric computations. In addition, it follows that the angle of misalignment of the zoom lens axis of symmetry can be computed from the principal point versus principal distance data. Measurements of the lens-image-plane misalignment angle for several solid-state cameras using this technique were typically less than 0.5 deg. Self-calibration simulations indicate that the asymmetrical decentering component of distortion due to the misalignment of the zoom lens is directly proportional to the symmetrical radial distortion component, the principal distance, and the angle of misalignment. Simulations which include decentering coefficients also indicate that for misalignment angles expected for zoom lenses and for reasonably large values of radial distortion the additional error introduced by ignoring the zoom lens misalignment may be only of the order of a few hundredths of a pixel, which at the current levels of accuracy is almost insignificant. The implications of this study are that special measures to properly align the zoom lens to the sensor image plane are probably not necessary, but that as the accuracy obtainable in digital photogrammetry approaches the 0.01 pixel or less level, the use of separate reference points for distortion and photogrammetric computations should be considered. For very large values of radial distortion or where justifiable in the error budget, explicit correction of the misaligned image plane via the proper 2-D projective transformation may be considered. The relations presented here should be useful in modeling of lens-image-plane misalignment, particularly for zoom lenses.

## 6. REFERENCES

1. A. G. Wiley and K. W. Wong, "Geometric calibration of zoom lenses for computer vision metrology," *PE&RS*, Vol. 61, No. 1, pp. 69–74, Jan. 1995.

2. R. G. Wilson, "Modeling and calibration of automated zoom lenses," *SPIE*, Vol. 2350, Videometrics III, pp. 170–186, Nov. 1994.

3. I. C. Gardner, "Relation of camera error to photogrammetric mapping," *J. of Research of the NBS*, Vol. 22, Research Paper RP1177, pp. 209–238, Feb. 1939.

4. D. C. Brown, "Application of close-range photogrammetry to measurements of structures in orbit volume 1," GSI TR 80-012 Sept. 1980.

5. C. C. Slama, *"Manual of Photogrammetry,"* 4th ed. ASP Falls Church, VA, 1980.

6. L. W. Fritz and H. H. Schmid, "Stellar Calibration of the Orbigon Lens," *PE&RS*, Vol. 40, pp.101–115, Jan. 1974.

7. A. W. Burner, W. L. Snow, M. R. Shortis, and W. K. Goad, "Laboratory calibration and characterization of video cameras," *SPIE*, Vol. 1395, Close-Range Photogrammetry Meets Machine Vision, Zurich, Switzerland, pp. 664–671, Sept. 3–7, 1990.

8. J. G. Fryer and Duane C. Brown, "Lens distortion for close-range photogrammetry," *PE&RS*, Vol. 52, No. 1, pp. 51–58, Jan. 1986.

9. A. E. Conrady, "Decentered lens-systems," *Roy. Astron. Soc.*, M.N. 79, pp. 384–390, March 1919.

10. D. Brown, "Decentering Distortion of Lenses," PE 32 (3), pp. 444–462, May 1966.
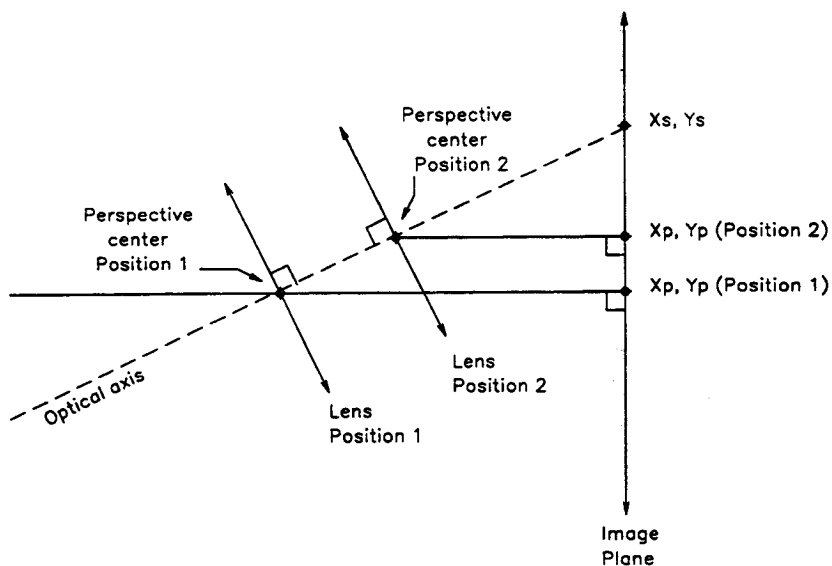
Fig. 1. Relationship of the principal point $(x_p, \ y_p)$ and the point of symmetry $(x_s, \ y_s)$.
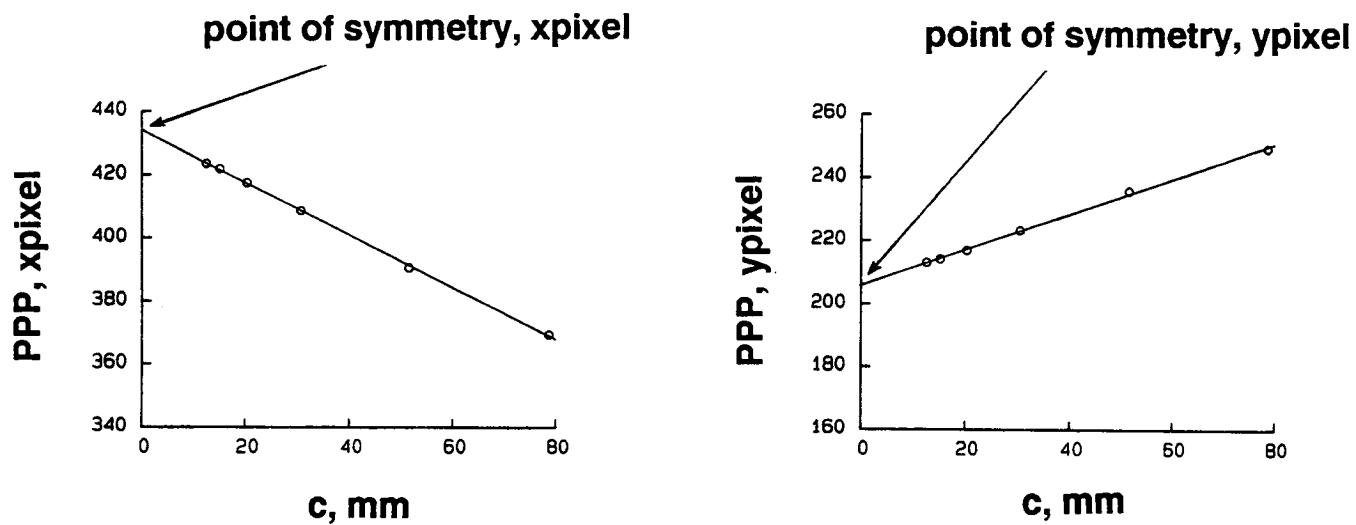


Fig. 2. Variation in the photogrammetric principal point (PPP) as a function of principal distance, $c$, and the location of the point of symmetry for a zoom lens.
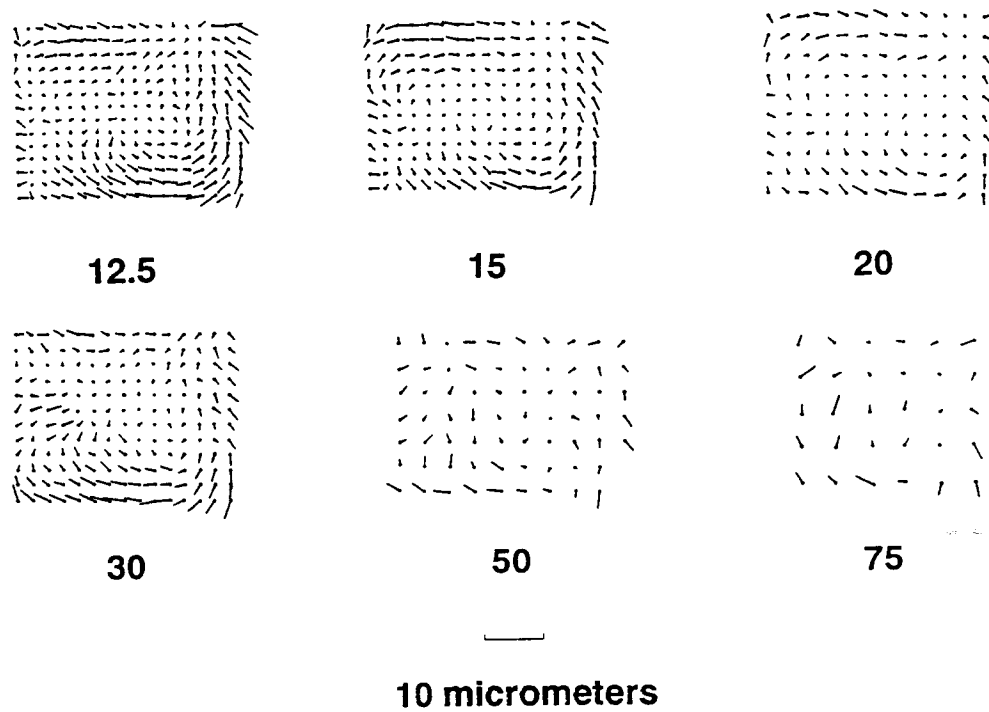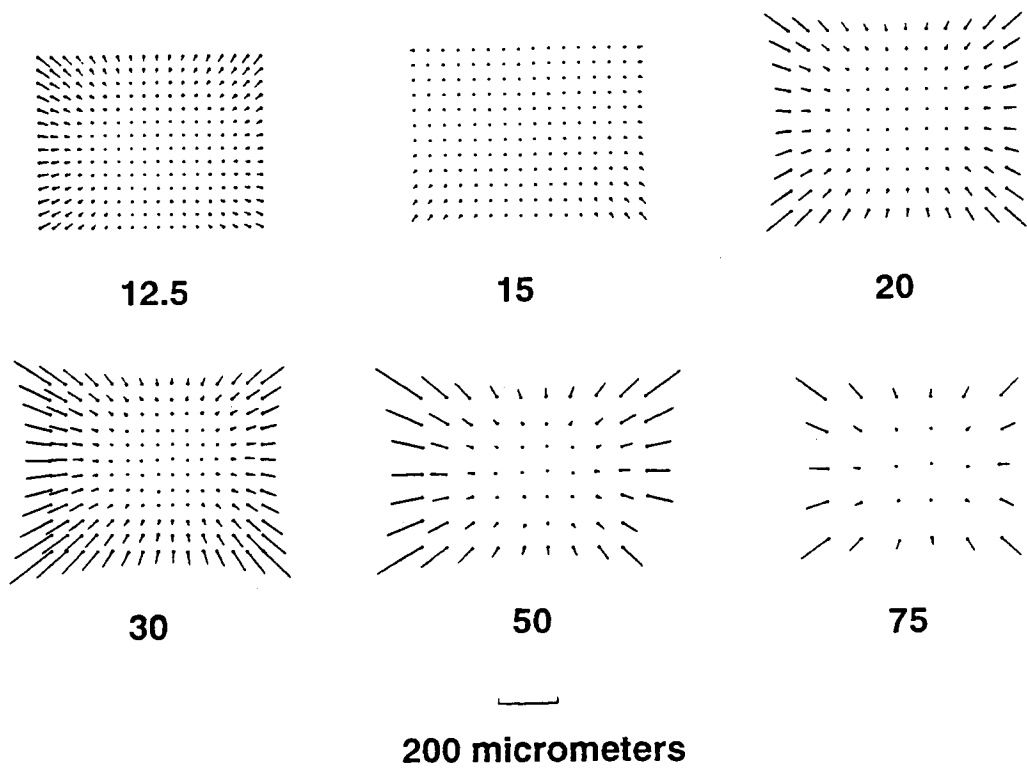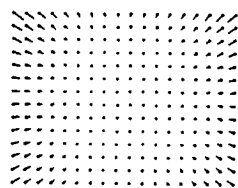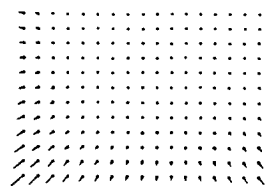
**12.5**          **15**          **20**

**30**          **50**          **75**

─────

**200 micrometers**

**12.5**          **15**          **20**

**30**          **50**          **75**

─────

**10 micrometers**

Fig. 3. Image plane residuals before (top) and after (bottom) distortion correction when the optical axis is perpendicular to the image plane.

**12.5**  **15**  **20**
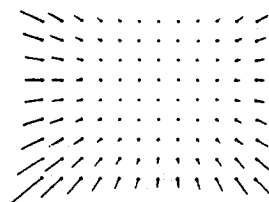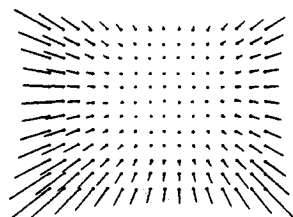
**30**  **50**  **75**
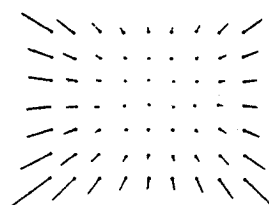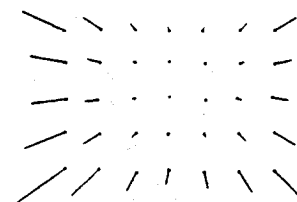
**200 micrometers**
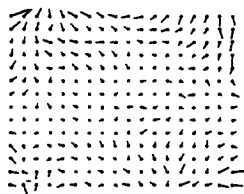
**12.5**  **15**  **20**
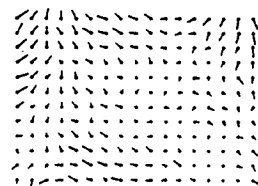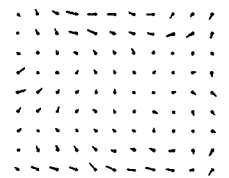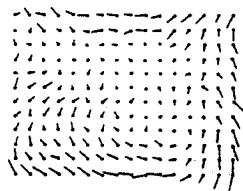
**30**  **50**  **75**
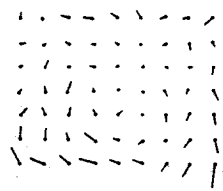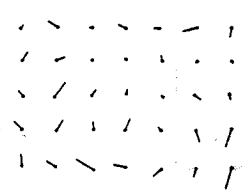
**10 micrometers**

Fig. 4. Image plane residuals before (top) and after (bottom) distortion correction when the optical axis is rotated from the image plane normal by 0.5 deg in the horizontal and vertical directions.
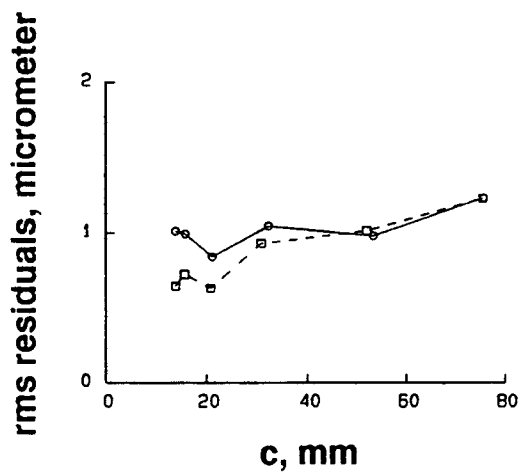
Fig. 5. Image plane residuals after distortion correction versus zoom setting. Circles denote the aligned case and squares denote the misaligned case.
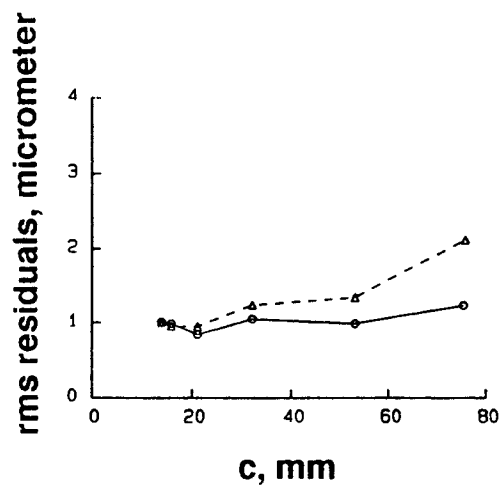
Fig. 6. Image plane residuals after distortion correction versus zoom setting for the aligned case comparing results using the experimentally determined point of symmetry (circles) and the nominal center of the image plane (triangles).
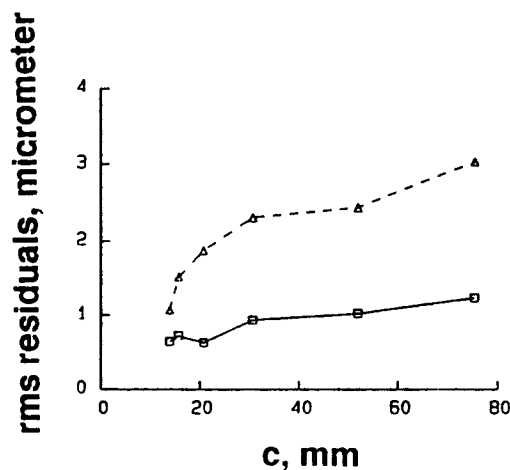


Fig. 7. Image plane residuals after distortion correction versus zoom setting for the misaligned case comparing results using the experimentally determined point of symmetry (squares) and the nominal center of the image plane (triangles).
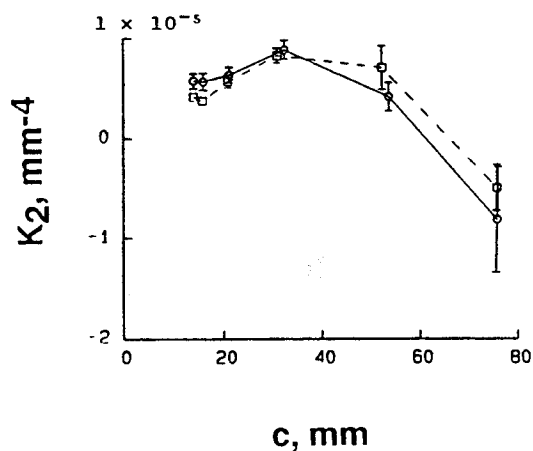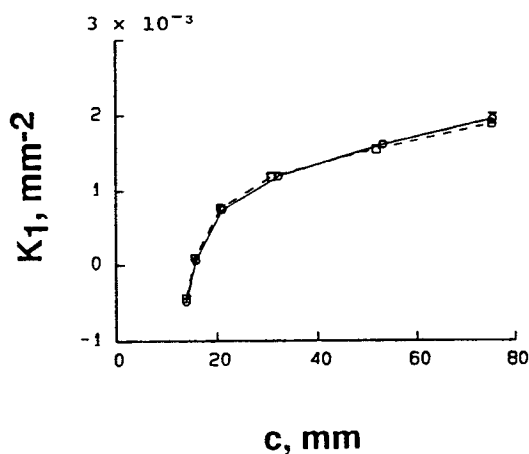


Fig. 8. Third $(K_1)$ and fifth $(K_2)$ order radial distortion terms versus zoom setting. Circles and squares represent the aligned and misaligned cases respectively.
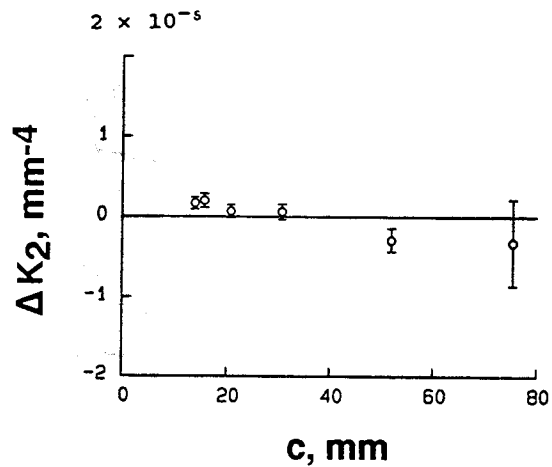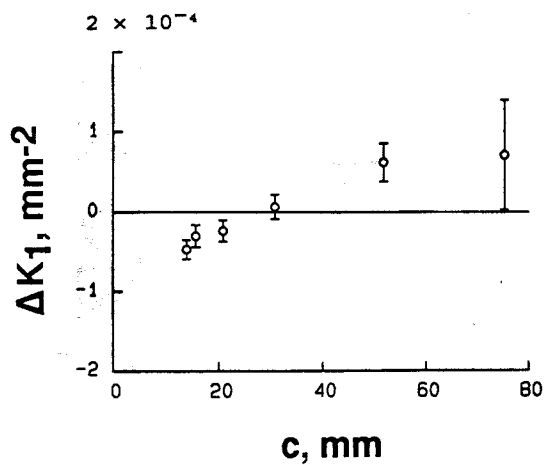
Fig. 9. Differences between aligned and misaligned cases versus zoom lens setting.
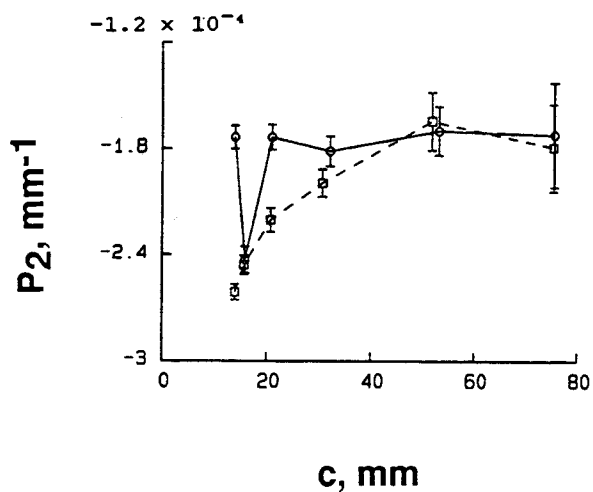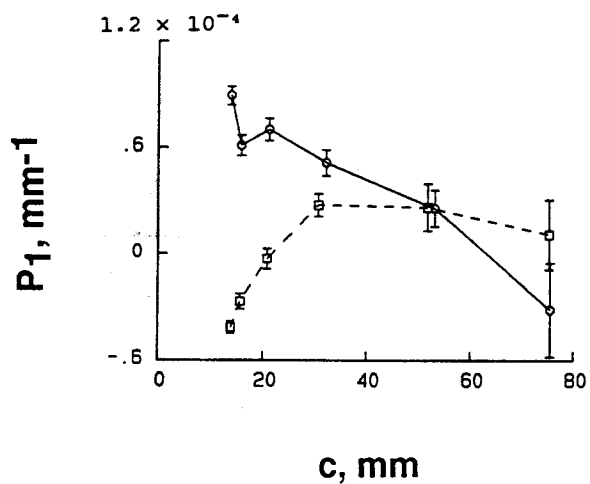


Fig. 10. Decentering distortion terms versus zoom setting. Circles and squares represent the aligned and misaligned cases respectively.
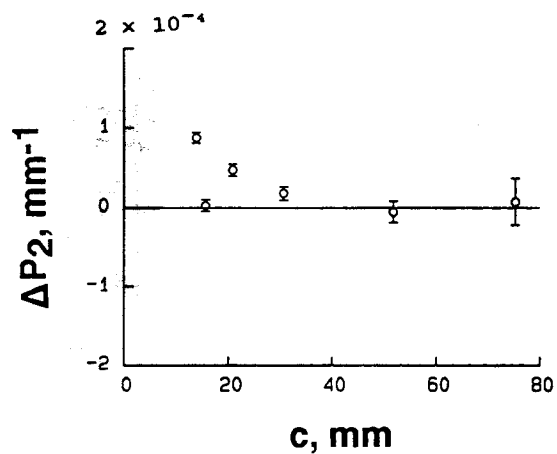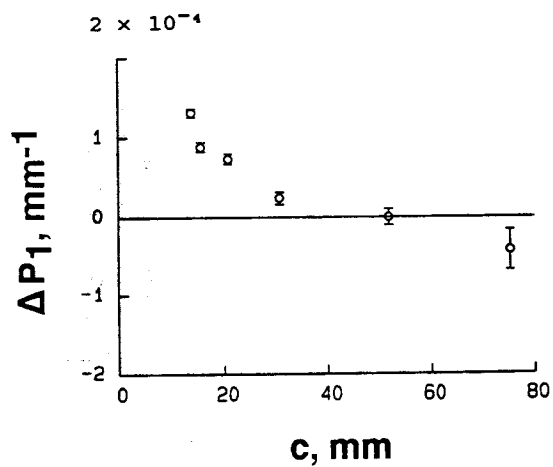


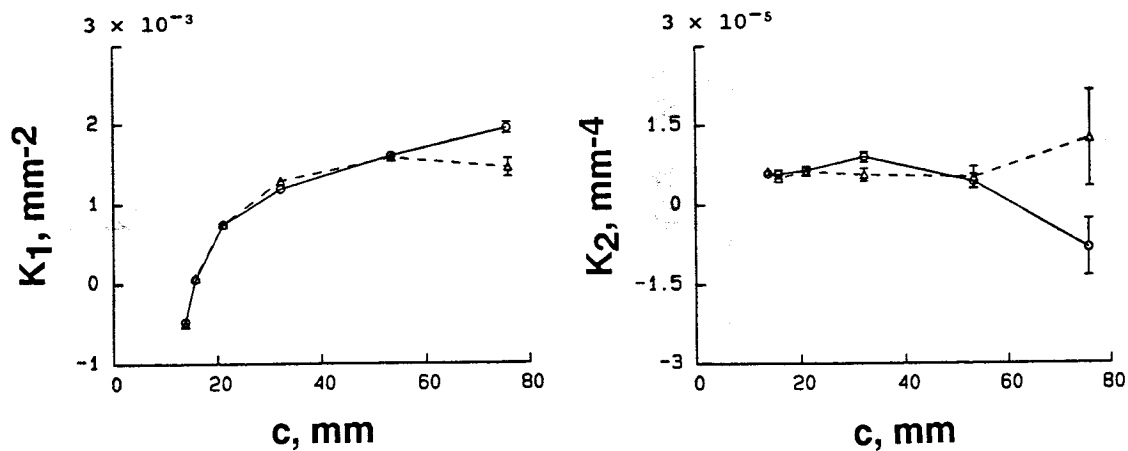Fig. 11. Differences between aligned and misaligned cases versus zoom lens setting.

Fig. 12. Radial distortion using the measured point of symmetry (circles) and the nominal center of the image plane (triangles) for distortion computations for the aligned case.
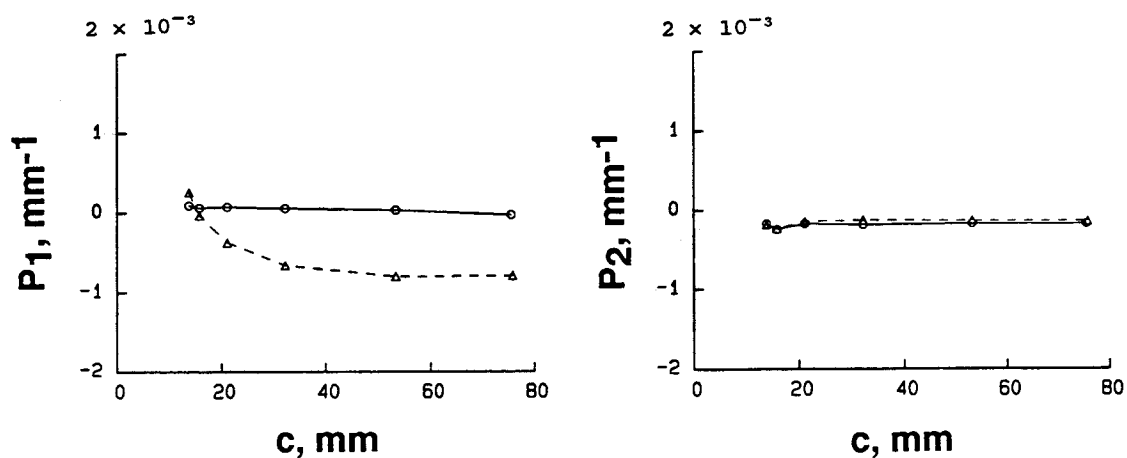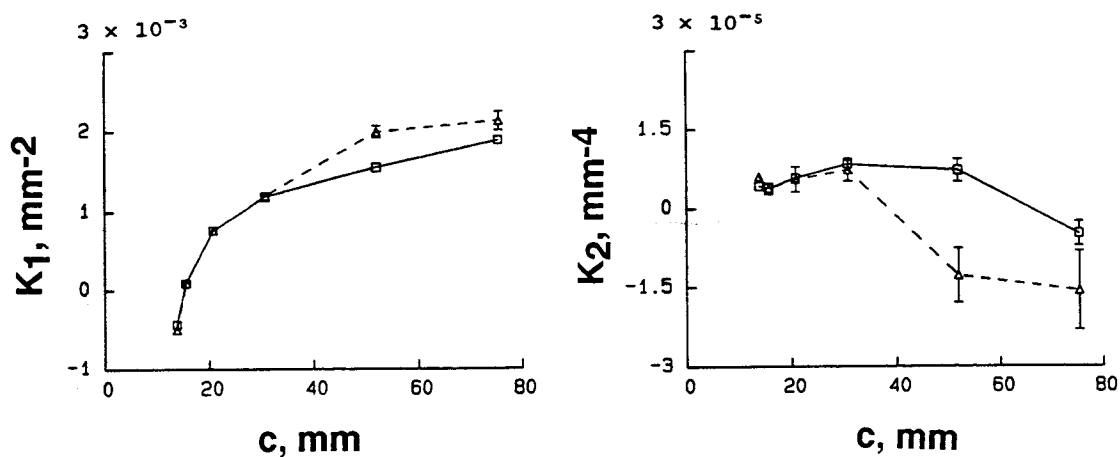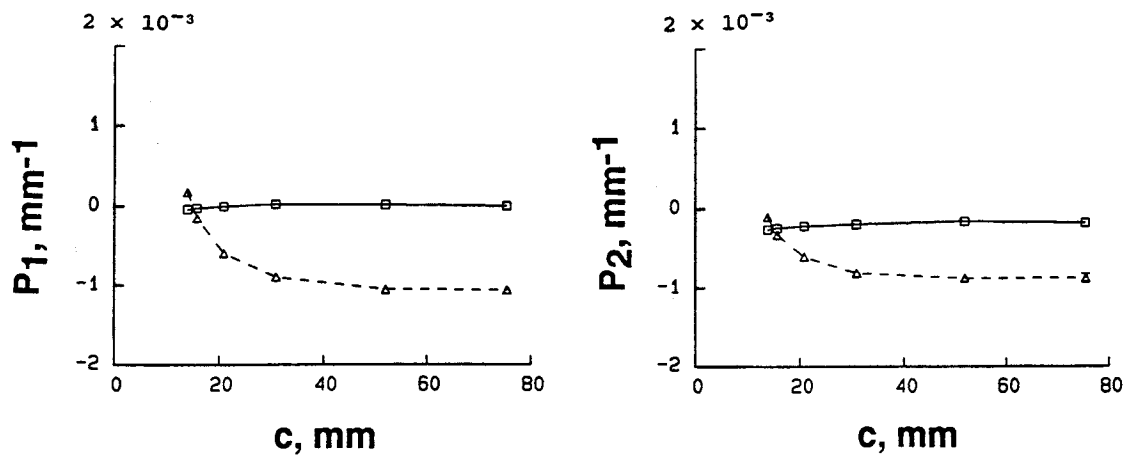


Fig. 13. Decentering distortion using the measured point of symmetry (circles) and the nominal center of the image plane (triangles) for distortion computations for the aligned case.



Fig. 14. Radial distortion using the measured point of symmetry (squares) and the nominal center of the image plane (triangles) for distortion computations for the misaligned case.

Fig. 15. Decentering distortion using the measured point of symmetry (squares) and the nominal center of the image plane (triangles) for distortion computations for the misaligned case.
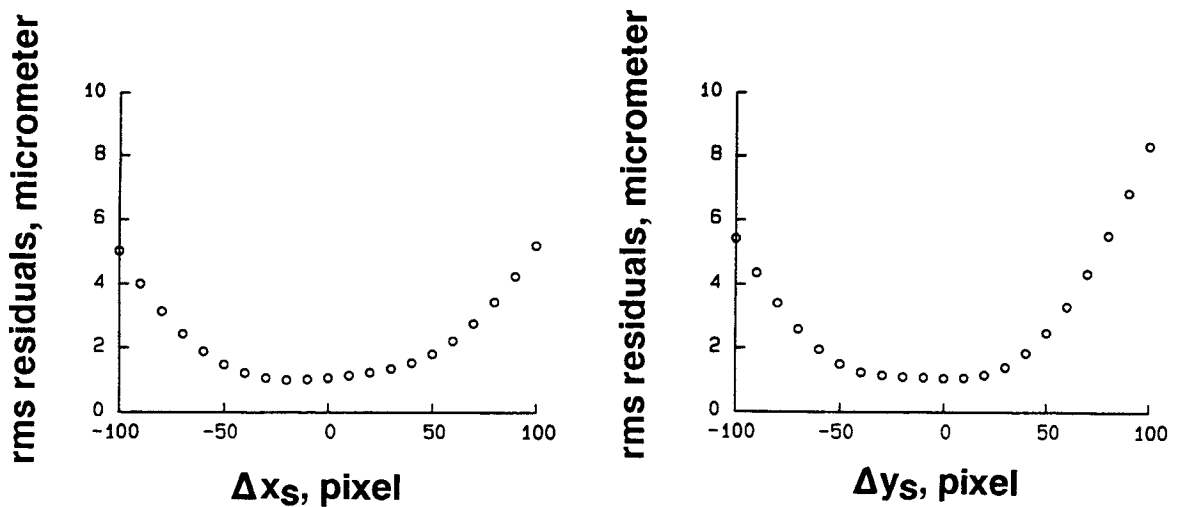


Fig. 16. Rms image plane residuals as a function of variations in the location of the point of symmetry for the aligned case.
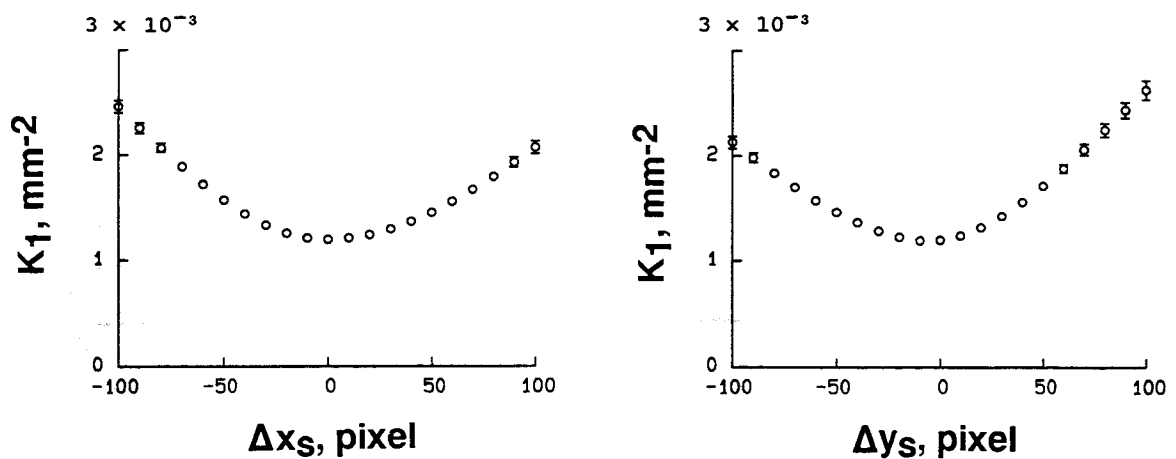


Fig. 17. Third order radial distortion as a function of variations in location of the point of symmetry for the aligned case.
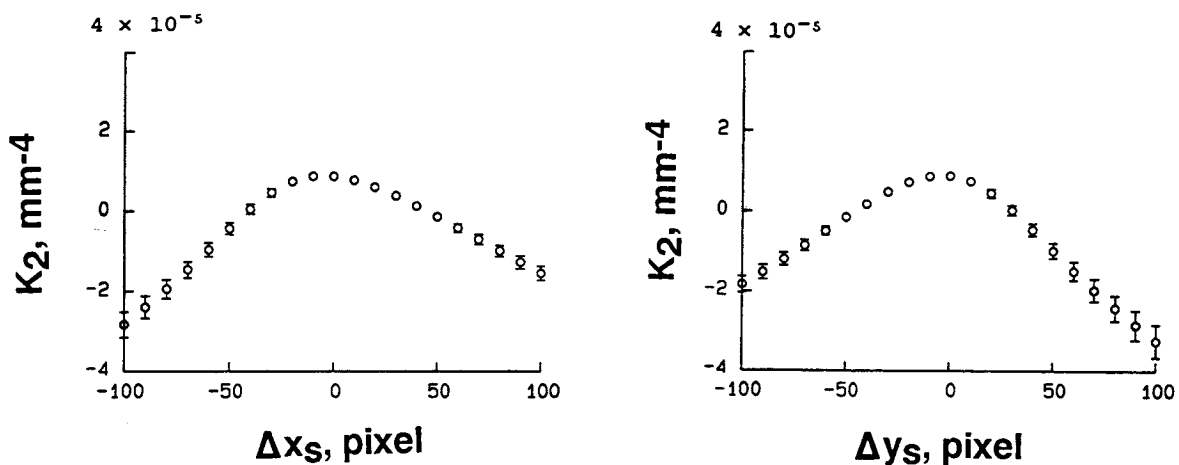
Fig. 18. Fifth order radial distortion as a function of variations in location of the point of symmetry for the aligned case.
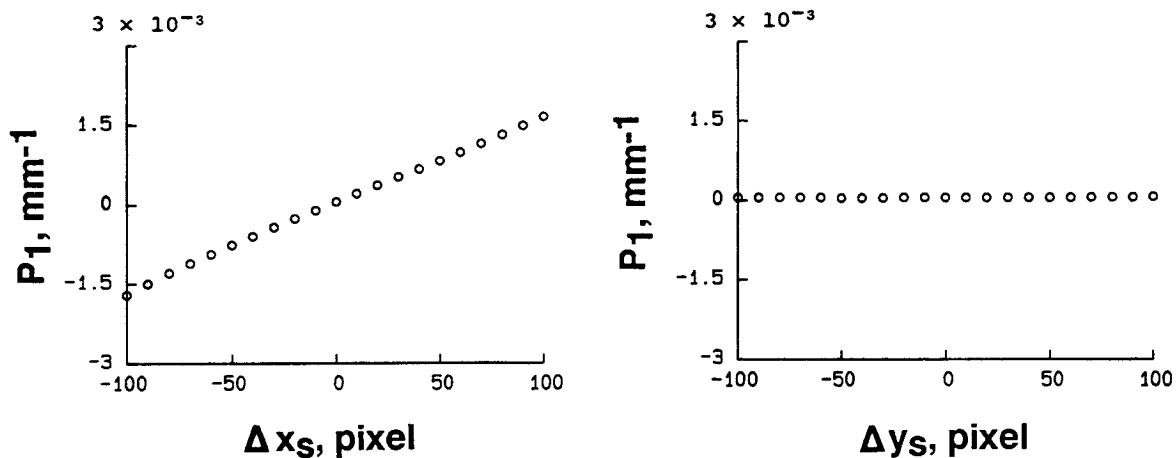


Fig. 19. Decentering distortion coefficient $P_1$ as a function of variations in location of the point of symmetry for the aligned case.
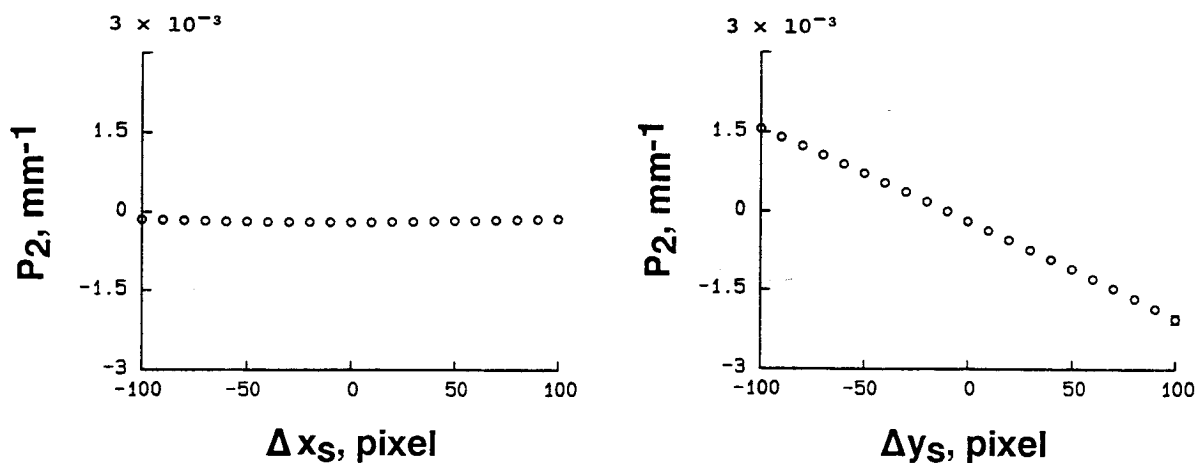


Fig. 20. Decentering distortion coefficient $P_2$ as a function of variations in location of the point of symmetry for the aligned case.